Organic & Biomolecular Chemistry

PAPER

View Article Online
View Journal | View Issue

Cite this: *Org. Biomol. Chem.*, 2014, **12**, 6634

Enhanced catalysis and enantioselective resolution of racemic naproxen methyl ester by lipase encapsulated within iron oxide nanoparticles coated with calix[8]arene valeric acid complexes

Serkan Sayin, Enise Akoz and Mustafa Yilmaz*

Received 21st May 2014,
Accepted 1st July 2014

DOI: 10.1039/c4ob01048e

www.rsc.org/obc

In this study, two types of nanoparticles have been used as additives for the encapsulation of *Candida rugosa* lipase *via* the sol–gel method. In one case, the nanoparticles were covalently linked with a new synthesized calix[8]arene octa valeric acid derivative (**C[8]-C$_4$-COOH**) to produce new calix[8]arene-adorned magnetite nanoparticles (**NP-C[8]-C$_4$-COOH**), and then **NP-C[8]-C$_4$-COOH** was used as an additive in the sol–gel encapsulation process. In the other case, iron oxide nanoparticles were directly added into the sol–gel encapsulation process in order to interact electrostatically with both **C[8]-C$_4$-COOH** and *Candida rugosa* lipase. The catalytic activities and enantioselectivities of two novel encapsulated lipases (**Enc-NP-C[8]-C$_4$-COOH** and **Enc-C[8]-C$_4$-COOH@Fe$_3$O$_4$**) in the hydrolysis reaction of racemic naproxen methyl ester were evaluated. The results showed that the activity and enantioselectivity of the lipase were improved when the lipase was encapsulated in the presence of calixarene-based additives. Indeed, the encapsulated lipases have an excellent rate of enantioselectivity, with E = 371 and 265, respectively, as compared to the free enzyme (E = 137). The lipases encapsulated with **C[8]-C$_4$-COOH** and iron oxide nanoparticles (**Enc-C[8]-C$_4$-COOH@Fe$_3$O$_4$**) retained more than 86% of their initial activities after 5 repeated uses and 92% with **NP-C[8]-C$_4$-COOH**.

Introduction

Researchers have developed various methods involving enzymatic and non-enzymatic catalysts to enrich a derivative for one of the enantiomers from the reaction product.[1–9] Biocatalysis has been applied as a viable and preferred technique in organic synthesis for the production of enantiopure compounds, particularly for pharmaceutical compounds.[10,11] *Candida rugosa* lipase has a wide range of natural substrates and is thus commonly chosen as a biocatalyst.[12] Moreover, lipases are usually used as aqueous solutions, which makes their recovery and reuse problematic and can also result in contamination of the product.[13] In an attempt to enhance the activity and enantioselectivity of *C. rugosa*, researchers have tried immobilizing *C. rugosa* using various types of carriers such as celite, kaolin, cyclodextrin, amberlite XAD 7, sporopollenin, chitosan, and calixarene.[14–16]

Recently, immobilizing the lipase using calixarenes has become a common way of increasing the lipase activity and enantioselectivity.[12,17,18] Calixarenes are used to this end because they are strong building blocks and maintain functionalization at both lower-rim and upper-rim positions.[19–24]

Over the past few years, scientists have grafted certain calixarene derivatives onto the surface of silica-modified-iron oxide nanoparticles in order to provide easier separation and more reusable processes. Furthermore, in order to improve the activity and enantioselectivity of lipases in the hydrolysis reaction of racemic naproxen methyl ester, some calixarene-grafted magnetite nanoparticles have successfully immobilized the lipase *via* the sol–gel method, which opens up a wide range of opportunities for future research.[14,25]

In the present study, *p-tert*-butylcalix[8]arene was substituted with valeric acid, and selectively grafted onto amino-silica-modified magnetite nanoparticles to afford the corresponding calix[8]arene-hepta acid-immobilized magnetite nanoparticles (**NP-C[8]-C$_4$-COOH**). The *C. rugosa* lipase was encapsulated within a sol–gel system[8,9,12,14,17,18] formed through polycondensation with tetraethoxysilane (TEOS) and octyltriethoxysilane (OTES) in the presence or absence of octa valeric acid functionalized calix[8]arene (**C[8]-C$_4$-COOH**) with magnetite nanoparticles to afford **Enc-C[8]-C$_4$-COOH@Fe$_3$O$_4$**. Moreover, **NP-C[8]-C$_4$-COOH** was also employed as an additive for the encapsulation of *C. rugosa* lipase to produce **Enc-C[8]-**

Department of Chemistry, Selcuk University, Konya-42075, Turkey.
E-mail: myilmaz42@yahoo.com; Fax: +90 332 2412499; Tel: +90 332 2233873

C_4-COOH. The activity and enantioselectivity of the encapsulated lipases were also evaluated under different conditions such as temperature and pH influences. The magnetite properties of these encapsulated lipases with nanoparticles provide easy separation with respect to reducing the labor force, as well.

Results and discussion

Synthesis of calixarene molecules

In our previous study,[26] we prepared an octa-acid derivative of *p-tert*-butylcalix[8]arene (**6**),[33] and examined its usability as an additive in the encapsulation of lipases *via* the sol–gel process.[1] To obtain **6**, *p-tert*-butylcalix[8]arene was treated with methylbromo acetate to synthesize its octa ester derivative (**5**). Upon hydrolysis, **5** yielded an octa-acid derivative of *p-tert*-butylcalix[8]arene (**6**)[26] (Scheme 1). The focus of the current study was to prepare two novel encapsulated lipases (**Enc-NP-C[8]-C_4-COOH** and **Enc-C[8]-C_4-COOH@Fe_3O_4**) in order to evaluate their catalytic and enantioselective properties. To this end, *p-tert*-butylcalix[8]arene was initially treated with 5-bromovalerate to afford the octa-valerate derivative **C[8]-C_4-COOEt** (**2**). The structure of **C[8]-C_4-COOEt** was confirmed not only by the appearance of a new vibration band at 1732 cm^{-1}, which is the carbonyl group of the ester derivative (**2**) on the FTIR spectrum, but also by the appearance of the peak at 1.11 ppm (24H, $-CH_3$) and the peaks of $-CH_2$ which came from the valerate groups on the ^{1}H-NMR spectrum. The octa-valeric acid derivatives of *p-tert*-butylcalix[8]arene (**C[8]-C_4-COOH**) (**3**) having a longer alkyl chain than **6** were synthesized by hydrolysis of **2** with an aqueous solution of NaOH for the first time (Scheme 1). The FTIR spectrum of **C[8]-C_4-COOH** clearly shows that the ester carbonyl vibration shifted to an acid carbonyl

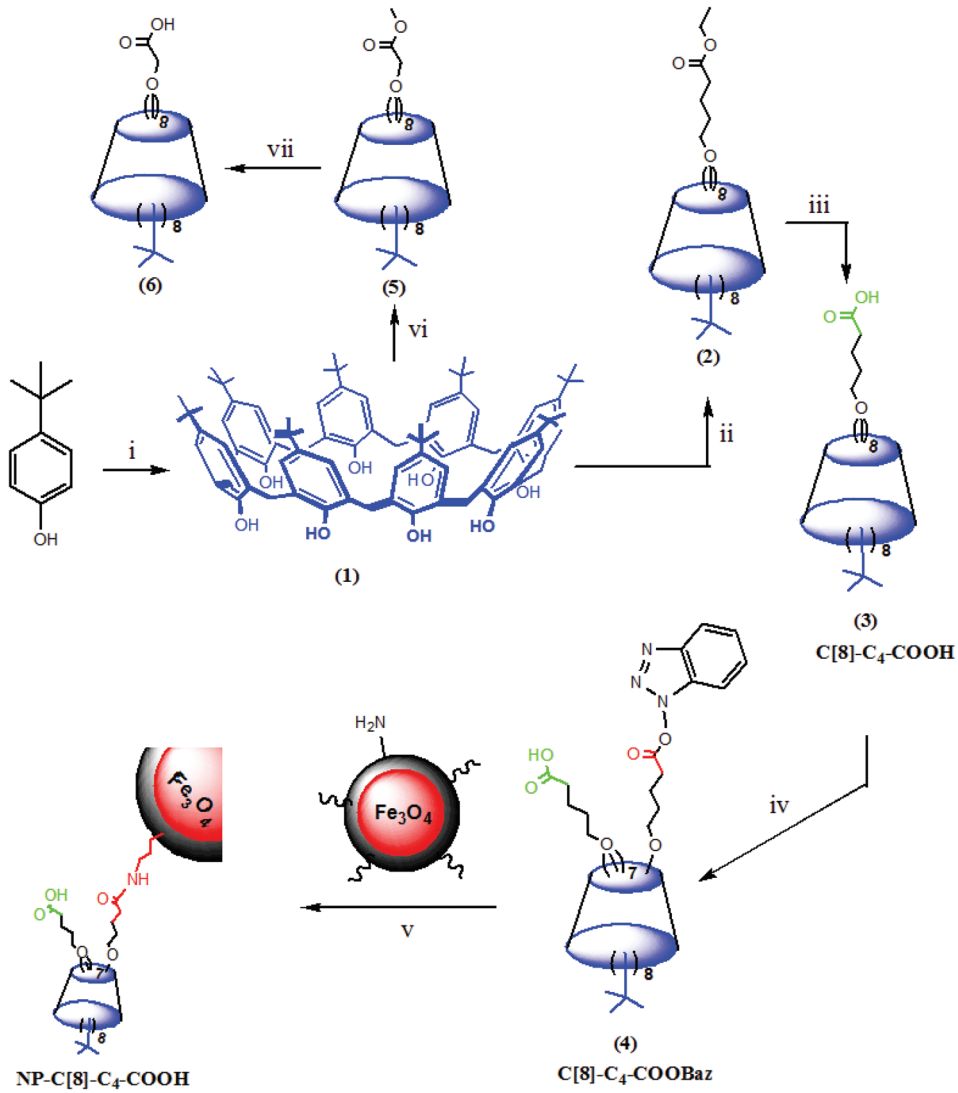

Scheme 1 Preparation of **C[8]-C_4-COOH** and **NP-C[8]-C_4-COOH**. Reaction conditions: (i) paraformaldehyde, NaOH; (ii) K_2CO_3, NaI, 5-bromovalerate; (iii) 15% NaOH solution; (iv) 1-hydroxybenzotriazole, DCC; (v) **Fe_3O_4-APTES**; (vi) methylbromoacetate, K_2CO_3; (vii) 15% NaOH solution.

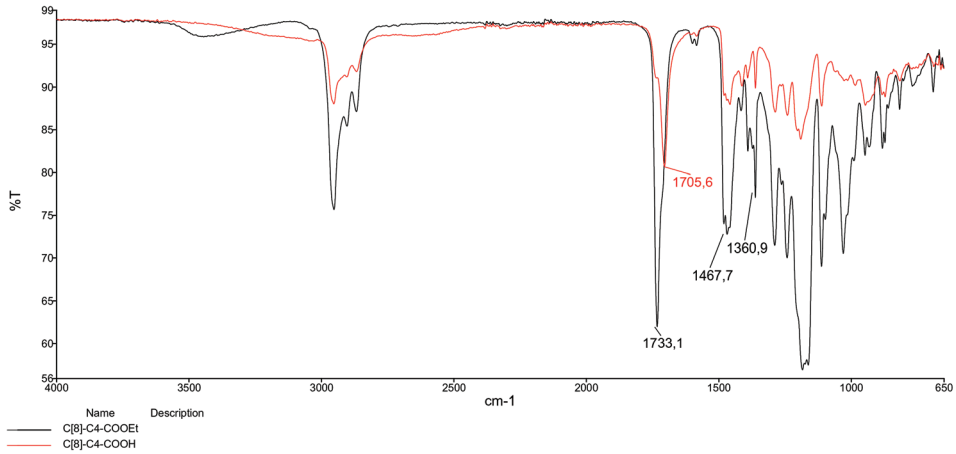

Fig. 1 FTIR spectra of **C[8]-C_4-COOEt** and **C[8]-C_4-COOH**.

vibration band at 1704 cm^{-1} (Fig. 1). The ^{1}H-NMR spectrum of **C[8]-C_4-COOH** also proves the structure of **3** by disappearance of the $-CH_3$ peak of **C[8]-C_4-COOEt**.

One acid moiety of **C[8]-C_4-COOH** (**3**) was selectively treated with 1-hydroxybenzotriazol to afford the corresponding 5,11,17,23,29,35,41,47-octa-*tert*-butyl-49-mono-(benzotriazol-1)-oxycarbonylbutoxy-50,51,52,53,54,55,56-hepta-hydroxycarbonyl butoxy-calix[8]arene (**C[8]-C_4-COOBaz**) (**4**) (Scheme 1). The ^{1}H-NMR spectra of **4** confirmed exclusive functionalization by giving the expected splitting pattern (two doublets at 7.69 and 7.96 ppm and two triplets at 7.39 and 7.52 ppm for 1 integral ratio proton of ArH of the benzotriazole unit). Subsequently, **C[8]-C_4-COOBaz** was grafted onto the aminosilica-modified Fe_3O_4 nanoparticles (**Fe_3O_4-APTES**), which were prepared according to the literature,[27] in order to produce **NP-C[8]-C_4-COOH** (Scheme 1). **NP-C[8]-C_4-COOH** was then used as an additive in the encapsulation of the lipase. FTIR spectra were used to elaborate the structure of **NP-C[8]-C_4-COOH** (Fig. 2). The characteristic peaks of **NP-C[8]-C_4-COOH** appeared at 1641 (COONa) and 1621 cm^{-1} (COONH). Additional peaks centered at 1542, 1468, 1413 and 1363 cm^{-1}, which are stretching vibrations of the aromatic C=C bonds of the calix[8]arene derivative. Moreover, the FTIR spectrum also shows peaks of the magnetite nanoparticles at 1149, 1046, 957 and 790 cm^{-1} for the Si–O group and at 578 cm^{-1} for the Fe–O group (see Fig. 2).

Transmission electron microscopy (TEM) analysis was used to obtain more information about particle size and morphology (see Fig. 3) of Fe_3O_4-nanoparticles (Fig. 3a), and **NP-C[8]-C_4-COOH** (Fig. 3b). TEM images of Fe_3O_4-nanoparticles are observed as intensive aggregates due to the lack of any repulsive force between the magnetite nanoparticles, which is due to a single magnetic crystallite and the uniform nano-size of the Fe_3O_4, which has a typical size range of 8 ± 3 nm and is surrounded by a silica-based material and calixarene units that are about 19 ± 5 nm thick. Using calix[8]arene derivative immobilization, the dispersion of particles was improved greatly (Fig. 3b) due to the production of an electrostatic repulsion force and steric hindrance between the calix[8]arene and the surface of the Fe_3O_4 nanoparticles.

Thermogravimetric analysis (TGA) was used to determine the amount of **C[8]-C_4-COOH** (Fig. 4) on the aminosilica-modi-

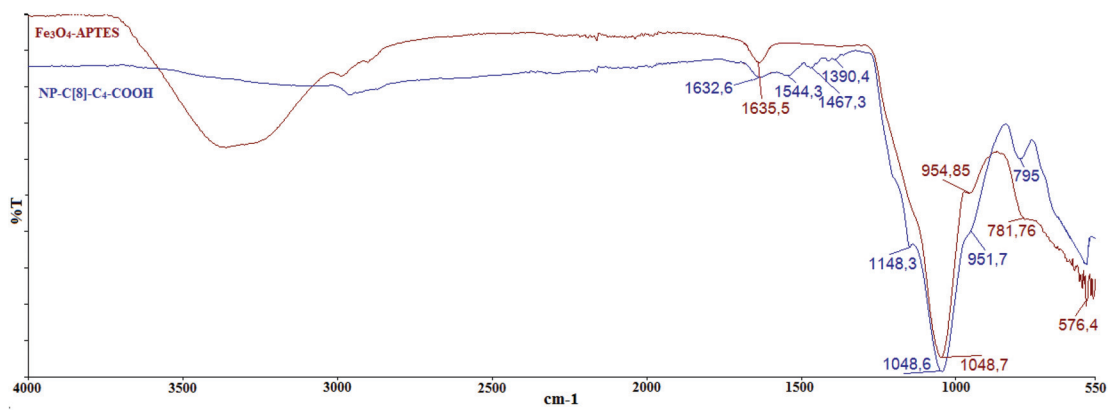

Fig. 2 FTIR spectra of **Fe_3O_4-APTES** and **NP-C[8]-C_4-COOH**.

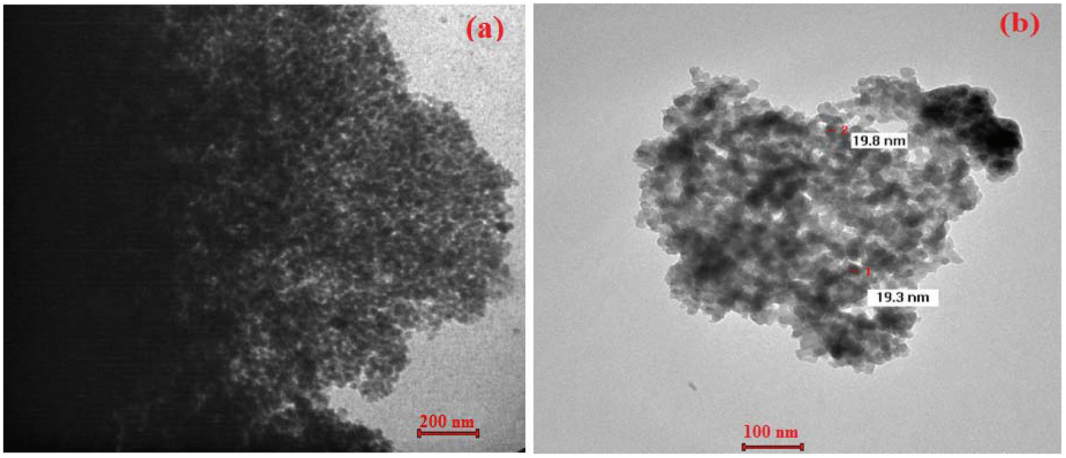

Fig. 3 TEM micrographs of (a) Fe_3O_4-nanoparticles and (b) **NP-C[8]-C_4-COOH**.

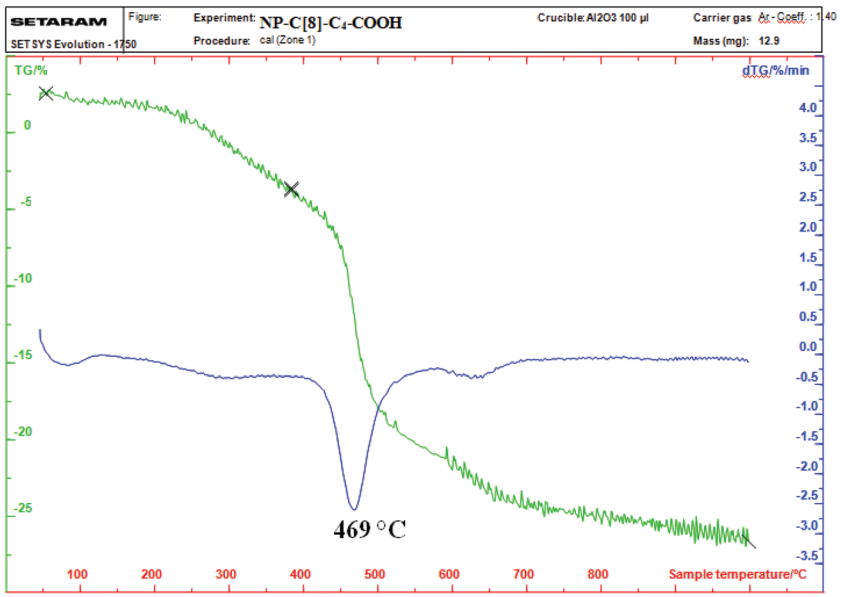

Fig. 4 TGA curves of **NP-C[8]-C_4-COOH**.

fied Fe_3O_4 nanoparticles (**Fe_3O_4-APTES**). As depicted in Fig. 4, the TGA curve of **NP-C[8]-C_4-COOH** reveals that the weight loss of 30% mass was due to the decomposition of **C[8]-C_4-COOH** and the 3-aminopropyltrimethoxysilane groups in the range of 325–625 °C.

Sol–gel procedure for the encapsulation of *C. rugosa* lipase on additives

In our previous study, calix[8]arene octa acid (**6**) was used as an additive in the sol–gel encapsulation process of lipases in order to estimate its catalytic ability in the enantioselective hydrolysis of racemic naproxen methyl ester.[26] It was found that the activity and enantioselectivity of the encapsulated lipase with **6** were extremely high when compared with the affinity of the encapsulated lipase without any additives.[26] This increase in activity and enantioselectivity of the lipase was attributed to a complex between the –COOH groups of the calix[8]arene derivative and the lysine moieties of the enzymes as well as host–guest interactions and the cooperative affinities of calix[8]arene derivatives.[18,26] The present study aimed to extend the number of calix[8]arene-based additives and compare their catalytic abilities. Furthermore, either a calix[8]-arene octa valeric acid derivative (**C[8]-C_4-COOH**) and Fe_3O_4-nanoparticles or hepta valeric acid-substituted calix[8]arene-grafted iron oxide nanoparticles (**NP-C[8]-C_4-COOH**) were employed as additives for the encapsulation of the lipase (see Fig. 5). A sol–gel procedure was used to encapsulate the lipase with or without additives, which provided mechanical entrapment of the enzyme according to the published procedure.[9,14,17] The Bradford method regarding bovine serum albumin was used as a standard to determine the amount of protein in the solution and in the elution solute.[28] The

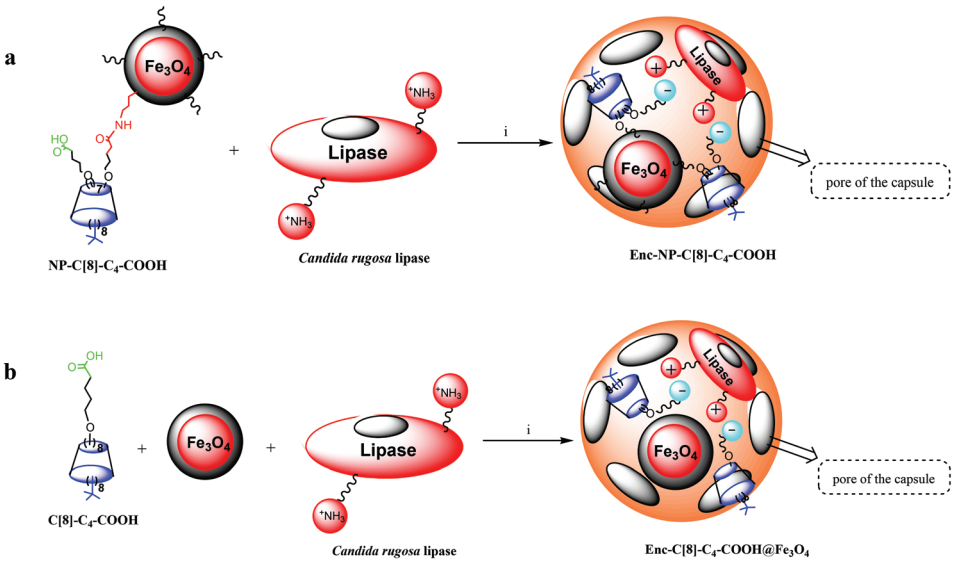

Fig. 5 Preparation of encapsulated lipases. Reaction conditions for (a and b); (i) phosphate buffer (pH 7.0), polyvinyl alcohol, NaF, isopropyl alcohol, tetramethoxysilane, octyltri-methoxysilane.

Table 1 Enantioselective hydrolysis of racemic naproxen methyl ester and activity of the encapsulated lipases under optimum reaction conditions

Lipase	Protein loading (mg g^{-1}-sol gel)	Lipase activity (Ug^{-1} sol gel)	Specific activity (U mg^{-1} protein)	Conversion (x, %)	ee_p (%)	E
Enc-lipase[a]	28.5	95	3.3	20	>98	137
Enc-C[8]-COOH[b]	26.8	37	1.4	30	>98	150
Enc-C[6]-COOH[c]	27.9	44	1.6	27	>98	141
Enc-C[4]COOH[d]	28.5	28	1.0	43	>98	224
Enc-Dibenzo-18-crown-6[e]	18.3	25	1.4	33	>98	193
Enc-NP[f]	33.0	102	3.1	30.7	>98	170
Enc-C[8]-C_4-COOH@Fe_3O_4[g]	22.0	35	1.6	49	>98	**371**
Enc-NP-C[8]-C_4-COOH[h]	15.5	43	2.8	46	>98	**265**

[a] *Candida rugosa* lipase encapsulated without calixarene or magnetite nanoparticles. [b] *Candida rugosa* lipase encapsulated with **C[8]-COOH**.[35] [c] *Candida rugosa* lipase encapsulated with **C[6]-COOH**.[35] [d] *Candida rugosa* lipase encapsulated with **C[4]-COOH**.[35] [e] *Candida rugosa* lipase encapsulated with **dibenzo-18-crown-6**.[17] [f] *Candida rugosa* lipase encapsulated with **NP**.[9] [g] *Candida rugosa* lipase encapsulated with **C[8]-C_4-COOH** and iron oxide nanoparticles. [h] *Candida rugosa* lipase encapsulated with **NP-C[8]-C_4-COOH**.

changes in activity of the encapsulated lipases were determined according to the literature.[29,30]

Table 1 reveals the results of the initial attempt to associate the catalytic activity of the encapsulated lipases in the presence/absence of C[8]-COOH, Fe_3O_4-nanoparticles, and **Enc-C[8]-C_4-COOH@Fe_3O_4**. As seen in Table 1, in terms of catalytic activity and enantioselectivity, the encapsulated lipase in the presence of C[8]-COOH (**6**) did not show higher affinity than the encapsulated lipase (**Enc-C[8]-C_4-COOH@Fe_3O_4**). However, the encapsulated lipase with C[8]-COOH (**6**) was more efficient than the encapsulated lipase (**Enc-Lipase**) in the absence of additives (see Table 1). Moreover, in order to determine the role of the Fe_3O_4-nanoparticles in this reaction, the lipase was encapsulated in the presence of only Fe_3O_4-nanoparticles as an additive. However, the encapsulated lipase with iron oxide nanoparticles exhibited less activity (see Table 1). These findings clearly suggest that both octa COOH-substituted calix[8]-arene derivatives represent complexibility toward the lipase such as host–guest, hydrogen bonding, and ionic interactions that might increase the activity and stability of the lipase.

Table 1 also indicates the catalytic activity results of the encapsulated lipase in the presence of **NP-C[8]-C_4-COOH**. The encapsulated lipase (**Enc-NP-C[8]-C_4-COOH**) provided high catalytic activity and enantioselectivity as compared to the **Enc-Lipase** and **Enc-NP**.

Effect of pH and temperature on the lipase activity

The hydrolysis of *p*-NPP by the encapsulated lipases was examined to assess their catalytic activity at various pHs (4.0–9.0). Finding an optimum pH for the encapsulated lipases is the optimal point, since it is well known that the conformational change of the enzyme results in a different catalytic activity when the pH of the media is changed. With that in mind, the various pHs were altered so that the encapsulated lipases would show the most efficient hydrolysis behaviour towards *p*-NPP. It was found that both free and encapsulated (**C[8]-**

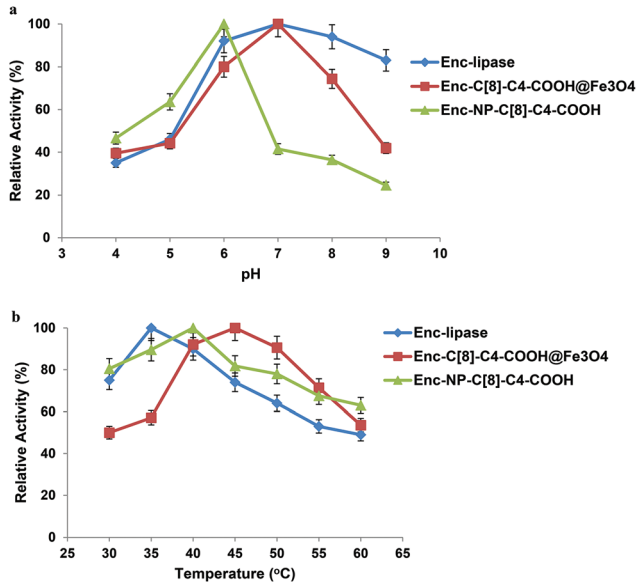

Fig. 6 (a) Effect of substrate pH on residual activity of the encapsulated lipases; (b) effect of reaction temperature on the residual activity of the encapsulated lipases. Averages and standard deviations calculated for data received from three independent extraction experiments.

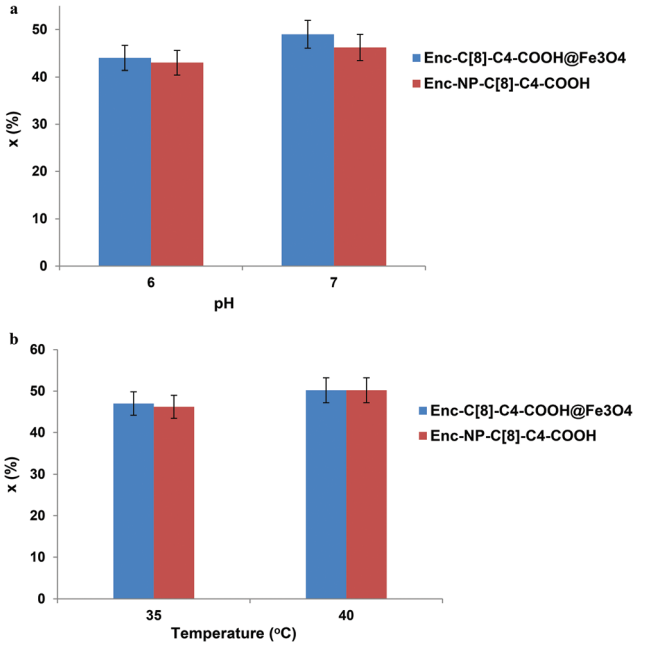

Fig. 7 Effect of pH (a) and temperature (b) on the conversion (*x*) in the hydrolysis of racemic naproxen methyl ester. Averages and standard deviations calculated for data received from three independent extraction experiments.

COOH, **C[8]-C4-COOH**) demonstrated high hydrolysis capability at pH 7.0, whereas the obtained efficient hydrolysis of *p*-NPP was observed to be at pH 6.0 for the encapsulated lipase in the presence of **NP-C[8]-C4-COOH** (see Fig. 6a).

To calculate the affinity of the encapsulated lipase (**Enc-Lipase**) without calixarene derivatives or magnetite nanoparticles, as well as the affinity of lipase-encapsulated calixarene derivatives with temperature, the reaction was carried out under various temperatures (30–60 °C) at pH 7.0 (Fig. 6b). It was observed that encapsulated lipases with **C[8]-C4-COOH** or magnetite nanoparticles showed high activity at 45 °C, whereas the highest activity of encapsulated lipases without additives was at 35 °C. The highest percentage depending upon the activity of **Enc-NP-C[8]-C4-COOH** was at 40 °C (see Fig. 6b). Immobilization shifted the optimum temperature from 35 °C for the free lipase to around 40–45 °C, due to either conformational limitations on enzyme movement as a result of multipoint interaction between the enzyme and the support or improved substrate diffusion at a high temperature. One of the main reasons for enzyme immobilization is the expected increase in stability toward various deactivating forces, due to the limited conformational mobility of the molecules after immobilization.[9,13,32]

Enantioselective hydrolysis of racemic naproxen methyl ester

Variations in pH and temperature can influence the conformation of the enzyme.[31] In an effort to visualise the effects of these parameters on the activity of the encapsulated lipase, we carried out the hydrolysis reaction of (*R*,*S*)-naproxen methyl ester at a pH range of 5–7 (see Fig. 7a) and at temperatures of 35 and 40 °C (see Fig. 7b).

In an earlier study, the interaction of encapsulated lipases with octa acid derivatives of calix[8]arene (**6**) *via* the sol–gel encapsulation method was employed as a catalyst for the enantioselective hydrolysis of the racemic naproxen methyl ester.[26] In order to understand and expand the range of encapsulated lipases available as enantioselective catalysts, in the present study, we describe two new encapsulated lipases (**Enc-NP-C[8]-C4-COOH** and **Enc-C[8]-C_4-COOH@Fe_3O_4**). In describing these new encapsulated lipases, we also aim to evaluate their chiral catalytic affinities.

The hydrolysis reaction results of (*R*,*S*)-naproxen methyl esters by the encapsulated lipases are shown in Table 1. After 24 h treatment of the encapsulated lipases with racemic naproxen methyl ester in aqueous buffer solution and isooctane, the lipases produced *R*-naproxen methyl ester and the corresponding acid (eep) >98%, the percentage of conversion (*x*) 49.0 for **Enc-C[8]-C_4-COOH@Fe_3O_4** and 46.0 for **Enc-NP-C[8]-C_4-COOH**. The treatment also resulted in enantioselectivities toward naproxen methyl ester (*E* value) of 371 for **Enc-C[8]-C_4-COOH@Fe_3O_4** and 265 for **Enc-NP-C[8]-C_4-COOH**, as compared to an *E* value of 137 for the encapsulated lipase without additives (**Enc-lipase**). These results show strong evidence that the immobilization of lipases with calixarene derivatives led to high stereoselectivity, high conversion, and fast recovery of the catalyst owing to the magnetite properties of the encapsulated lipases (**Enc-C[8]-C_4-COOH@Fe_3O_4** and/or **Enc-NP-C[8]-C_4-COOH**). This is not a surprising result, considering not only the highly effective complexing agent properties of the free –COOH groups of **C[8]-C_4-COOH** and **NP-C[8]-C_4-COOH** by means of forming salt bridges with lysine groups of

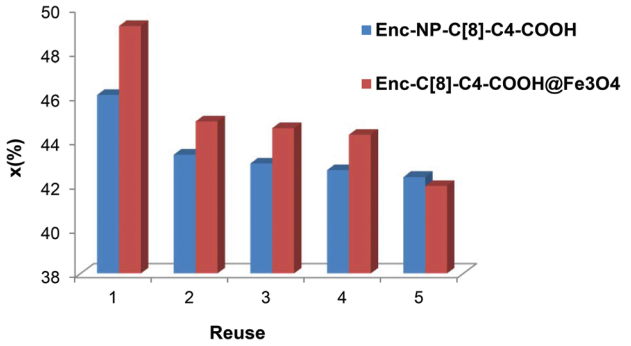

Fig. 8 Reusability on the conversion (*x*) in the hydrolysis of racemic naproxen methyl ester.

lipase, but also the host–guest interaction ability of calix[8]-arene. A considerable increase in the activity and enantioselectivity of the encapsulated lipase in the presence of additives has also been observed in the literature.[8,14,26,32]

Increasing the recovery and reusability of the enzyme is essential for economical usage. In this sense, the encapsulated lipases with their unique magnetite properties should be paid much attention because of their easy separability with a simple magnet. Fig. 8 shows that, even after the 5th reuse cycle, the encapsulated lipases still retained 42% of their conversion ratios for **Enc-C[8]-C_4-COOH@Fe_3O_4** and 42.4% for **Enc-NP-C[8]-C_4-COOH**.

Conclusion

We have synthesized a new *p-tert*-butylcalix[8]arene derivative (**C[8]-C_4-COOH**) and grafted it onto iron oxide nanoparticles to afford **NP-C[8]-C_4-COOH**. Both **C[8]-C_4-COOH** and Fe_3O_4-nanoparticles were used as additives for the encapsulation of lipase. Moreover, **NP-C[8]-C_4-COOH** was also used as an additive for the lipase encapsulation in order to form a salt bridge between lysine moieties of the enzyme and free COOH groups of calix[8]arene derivatives, as well as to provide an easy way out for the separation processes. Two new encapsulated lipases (**Enc-C[8]-C_4-COOH@Fe_3O_4** and **Enc-NP-C[8]-C_4-COOH**) were examined for the enantioselective hydrolysis of (*R*,*S*)-naproxen methyl ester. In addition, the effects of some parameters such as pH and temperature were also investigated. It was found that the enantioselectivity of (*R*,*S*)-naproxen methyl ester improved more with **Enc-C[8]-C_4-COOH@Fe_3O_4** and **Enc-NP-C[8]-C_4-COOH** than with the encapsulated lipase (**Enc-lipase**), with *E* values of 371 and 265, respectively. These findings demonstrate that the octa valeric acid-substituted calix[8]-arene derivatives are useful supports for lipase encapsulation. Hence, an approach is opened for developing a new technique to regulate enantioselective studies. Moreover, due to the low price of sol–gel encapsulation, the excellent performance of the lipase-immobilization, and its ready recyclability, the method is industrially workable.

Experimental

Reagents

DC Alufolien Kieselgel 60 F_{254} (Merck) was used for TLC analysis. All chemical reagents and starting materials, and all solvents were purchased from Aldrich, Fluka and Merck. HPLC grade organic solvents were used as the mobile phase without further purification or drying. A Millipore milli-Q Plus water purification system was used to receive deionized water. *Candida rugosa*, Bradford reagent, bovine serum albumin (99%), and *p*-nitrophenyl palmitate (*p*-NPP) were bought from Sigma Chemical Co. (St. Louis, MO).

Apparatus

A Varian 400 MHz spectrometer was used for NMR applications. FTIR spectra were evaluated on a Perkin Elmer spectrum 100 FTIR spectrometer. A Shimadzu 160A UV-visible recording spectrophotometer was used for UV-vis spectra. Thermogravimetric analysis (TGA) was carried out with a Seteram Evolution-1750 thermogravimetric analyzer. It was performed under an argon atmosphere. Transmission electron microscopy (TEM) analysis was carried out with FEI Tecnai G2 Spirit. Melting points were determined on an EZ-Melt apparatus in a sealed capillary. An Orion 410A+ pH meter was used for the pH measurements. High-performance liquid chromatography (HPLC) (Agilent 1200 Series) was carried out using a 1200 model quaternary pump, a G1315Bmodel diode array and multiple wavelength UV-vis detector, a 1200 model standard and preparative autosampler, a G1316A model thermostated column compartment, a 1200 model vacuum degasser, and an Agilent Chemstation B.02.01-SR2 Tatch data processor. The concentrations of *S*- and *R*-enantiomers of naproxen methyl ester were measured by HPLC (Agilent 1200 Series) using a Chiralcel OD-H column at a temperature of 25 °C. In the analysis, *n*-hexane–2-propanol–trifluoro acetic acid (100/1/0.1, v/v/v) was used as the mobile phase at a flow rate of 1 mL min^{-1}; and UV detection was done at 254 nm.

Synthesis

p-tert-Butylcalix[8]arene (**1**), Fe_3O_4 nanoparticles (**3**) and aminosilica-modified Fe_3O_4 nanoparticles (**Fe_3O_4-APTES**) were synthesized according to the literature.[14,27,33] The syntheses of octa ester derivatives of *p-tert*-butylcalix[8]arene (**2**), 5,11,17,23,29,35,41,47-octa-*tert*-butyl-49,50,51,52,53,54,55,56-octahydroxycarbonylbutoxy-calix[8]arene (**3**), 5,11,17,23,29,35,41,-47-octa-*tert*-butyl-49-mono-(benzotriazol-1)-oxycarbonylbutoxy-50,51,52,53,54,55,56-heptahydroxycarbonylbutoxy-calix[8]arene (**C[8]-C_4-COOBaz**) (**4**), and immobilization of **C[8]-C_4-COOBaz** onto aminosilica-modified iron oxide nanoparticles (**NP-C[8]-C_4-COOH**) are reported for the first time.

Synthesis of 5,11,17,23,29,35,41,47-octa-*tert*-butyl-49,50,51,-52,53,54,55,56-octaethoxycarbonylbutoxy-calix[8]arene (C[8]-C_4-COOEt) (2). A mixture of *p-tert*-butylcalix[8]arene (1 g, 0.771 mmol), K_2CO_3 (3.41 g, 24.672 mmol), NaI (1.85 g, 12.336 mmol) and 5-bromovalerate (24.672 mmol) in 90 mL of acetone was heated at 80 °C. The reaction was monitored

using TLC. After 5 days, the reaction was cooled to room temperature, filtered off, and the filtrate was evaporated to dryness. The remaining solid was dissolved in 100 mL Et_2O and washed with water to adjust to pH 7.0. The organic phase was dried over $MgSO_4$ and then filtered. The filtrate was evaporated under reduced pressure. The crude residue was recrystallized from MeOH. Yield 78.2%, M.p. 165–166 °C. FTIR (ATR): 1732 cm^{-1}(C═O). ^{1}H NMR ($CDCl_3$): δ 1.05 (s, 72H, Bu^t), 1.11 (t, 24H, J = 6.8 Hz, –CH_3), 1.72–1.76 (m, 32H, –CH_2–), 2.27 (t, 16H, J = 6.8 Hz, –CH_2–CO), 3.63 (brs, 16H, ArCH_2–Ar), 3.99–4.04 (m, 32H, ArO–CH_2– and O–CH_2–), 6.92 (s, 16H, ArH). ^{13}C-NMR (100 MHz, $CDCl_3$): δ (ppm) 14.21 (–CH$_3$), 21.62 (–CH$_2$), 29.66 (–CH$_2$), 31.26 (–CH$_3$ of Bu^t), 31.39 (Ar–CH$_2$–Ar), 31.59 (–C(CH$_3$)$_3$), 34.10 (–CH$_2$), 60.15 (O–CH$_2$–CH$_3$), 73.40 (O–CH$_2$), 125.90 (ArC), 132.95 (ArC), 145.83 (ArC), 150.58 (ArC–O), 173.41 (C═O). Anal. Calcd for $C_{144}H_{208}O_{24}$: C, 74.45; H, 9.02. Found (%); C, 74.51; H, 8.98.

Synthesis of 5,11,17,23,29,35,41,47-octa-*tert*-butyl-49,50,51,52,53,54,55,56-octahydroxycarbonylbutoxy-calix[8]arene (C[8]-C$_4$-COOH) (3). A solution of NaOH (15%) was added to a mixture of **C[8]-C$_4$-COOEt** (0.5 g, 0.43 mmol) in 50 mL EtOH. The reaction mixture was refluxed for 17 h. Then, the volatile component was evaporated, and the remaining solid was treated with cold water (50 mL) and HCl (3 N, 100 mL). The collected product was neutralized with water, and dried in an oven. Yield 88.5%; m.p. 294–296 °C. FTIR: 1704 cm^{-1} (C═O, acid). ^{1}H-NMR (DMSO-d_6): δ 0.94 (s, 72H, Bu^t), 1.60–1.65 (m, 32H, –CH_2–), 2.19 (t, 16H, J = 6.8 Hz, –CH_2–CO), 3.36–3.61 (m, 16H, Ar–CH_2–Ar), 3.93 (brs, 16H, ArO–CH_2–), 6.83 (s, 16H, ArH). ^{13}C-NMR (100 MHz, DMSO-d_6): δ (ppm) 22.18 (–CH$_2$), 29.52 (–CH$_2$), 29.88 (–CH$_3$), 31.51 (Ar–CH$_2$–Ar), 34.15 (–C(CH$_3$)$_3$), 34.67 (–CH$_2$), 72.82 (O–CH$_2$), 125.61 (ArC), 133.03 (ArC), 145.28 (ArC), 153.24 (ArC–O), 175.30 (C═O). Anal. Calcd for $C_{128}H_{176}O_{24}$: C, 73.25; H, 8.45. Found (%); C, 73.17; H, 8.48.

Synthesis of 5,11,17,23,29,35,41,47-octa-*tert*-butyl-49-mono-(benzotriazol-1)-oxycarbonylbutoxy-50,51,52,53,54,55,56-heptahydroxycarbonylbutoxy-calix[8]arene (C[8]-C$_4$-COOBaz) (4). To a solution of **C[8]-C$_4$-COOH** (0.3 g, 0.286 mmol) and 1-hydroxybenzotriazol (0.046 g, 0.34 mmol) in 25 mL THF was added DCC (0.071 g, 0.34 mmol), and then allowed to be stirred at rt for 48 h. The reaction was monitored using TLC. The solvent was then evaporated, and the residue was treated with EtOAc. The filtrate was evaporated to afford the final product. Yield 92%, ^{1}H NMR (DMSO): δ 0.94–1.03 (m, 72H, Bu^t), 1.57–1.71 (m, 34H, –CH_2– and –CH_2–CO), 2.16–2.19 (m, 14H, –CH_2–CO), 3.29–3.58 (m, 16H, ArCH_2–Ar), 3.93 (brs, 16H, ArO–CH_2–), 6.84–6.99 (m, 16H, ArH), 7.39 (t, 1H, J = 8.0 Hz, ArH), 7.52 (t, 1H, J = 7.2 Hz, ArH), 7.69 (d, 1H, J = 8.8 Hz, ArH), 7.96 (d, 1H, J = 8.8 Hz, ArH). Anal. Calcd for $C_{134}H_{179}N_3O_{24}$: C, 72.63; H, 8.14; N, 1.90. Found (%); C, 72.69; H, 7.94; N, 1.92.

Preparation of NP-C[8]-C$_4$-COOH

A mixture of **C[8]-C$_4$-COOBaz** (0.25 g) and **Fe$_3$O$_4$-APTES** (0.2 g) in 40 mL THF–DMF (v/v) was stirred at rt for 4 days. Then, **NP-C[8]-C$_4$-COOH** was collected using a simple magnet, and washed with THF, EtOH and H_2O, respectively. The product was dried in a vacuum oven. FTIR (KBr, cm^{-1}); 1641 (COONa), 1621 (COONH), 1542, 1468, 1413 and 1363 (C═C), 1149, 1046, 957 and 790 (Si–O), and 578 (Fe–O).

Sol–gel encapsulation of lipase with/without C[8]-C$_4$-COOH and magnetite nanoparticles or NP-C[8]-C$_4$-COOH

The method of Reetz was modified for sol–gel encapsulation of the lipases.[1] Typically, a mixture of lipase powder (lyophilizate) such as CRL-type VII (245 mg) in phosphate buffer (1.56 mL, 50 mM) adjusted at pH 7.0 was vigorously shaken. Either **NP-C[8]-C$_4$-COOH** (0.2 g) or **C[8]-C$_4$-COOH** (**3**) (0.1 g) and Fe_3O_4 (0.1 g) was added to the mixture, together with 400 μL of polyvinyl alcohol (4% w/v), 200 μL of NaF solution (0.1 M) and 400 μL of isopropyl alcohol. After obtaining homogeneity, tetramethoxysilane (460 μL, 0.5 mmol) and octyltrimethoxysilane (3.2 mL, 2.5 mmol) were added and left to be shaken for 10–15 s. Then, 15 mL of isopropyl alcohol was poured onto the dried white solid. The gel was washed with water (10 mL) and isopropyl alcohol (10 mL), and then it was lyophilized to produce the encapsulated lipases.

Lipase activity and protein assay determination

p-NPP in an aqueous phosphate buffer (100 mmol sodium phosphate, pH 7.0) was used to determine the hydrolytic activities of the encapsulated lipases. A UV-visible spectrophotometer was scanned at 410 nm in order to measure the concentration of the corresponding *p*-nitrophenol.[29,30]

Protein content was defined by the method of Bradford[28] using a Bio-Rad protein dye reagent concentrate. Bovine serum albumin was used as the standard.

pHs and temperatures on activity

Activity was determined between pH 4 and 9 in 50 mM phosphate buffer to see the changes in activity of free and immobilized lipases.[28–30] Moreover, the thermal inactivation of the free and immobilized lipases was investigated at 30–60 °C. Both forms of enzymes were incubated in PBS (50 mM, pH 7.0) for 20 min at various temperatures and, after lowering the temperature, the remaining activity was assayed under the standard conditions and analyzed.

Thermal stability

Each encapsulated lipase (with or without additives) was stored in the buffer (50 mM, pH 7.0) at 60 °C for 2 h, in order to estimate their activity as outlined above.

Enantioselective hydrolysis of racemic naproxen methyl ester by encapsulated lipases

A reaction system in an aqueous phase/organic solvent was used for the hydrolysis reactions according to the literature procedure.[8,12,14] The conversion and enantioselectivity of naproxen methyl ester by the encapsulated lipases in the presence or absence of additives such as either **C[8]-C$_4$-COOH** (**3**) and **Fe$_3$O$_4$**, or **NP-C[8]-C$_4$-COOH** were expressed as the enantiomeric ratio (E), which was calculated from the conversion (x)

and the enantiomeric excess of the substrate (ee_s) and the product (ee_p) using HPLC.[34]

$$E = \frac{\ln[(1-x)(1-ee_s)]}{\ln[(1-x)(1+ee_s)]}$$

$$x = \frac{ee_s}{ee_s + ee_p} \quad ee_s = \frac{C_R - C_S}{C_R + C_S} \quad ee_p = \frac{C_S - C_R}{C_S + C_R}$$

E, ee_s, ee_p, x, C_R and C_S stand for enantiomeric ratio for irreversible reactions, enantiomeric excess of substrate, enantiomeric excess of the product, racemate conversion, concentration of *R*-enantiomer and concentration of *S*-enantiomer, respectively.

Acknowledgements

This work was funded by the Scientific and Technological Research Council of Turkey (TUBITAK grant no.111T027 and CMST COST Action CM1005), and the Research Foundation of Selcuk University (BAP).

Notes and references

1 M. T. Reetz, P. Tielmann, W. Wisenhofer, W. Konen and A. Zonta, *Adv. Synth. Catal.*, 2003, **345**, 717–728.
2 M. Chen and W. R. Roush, *J. Am. Chem. Soc.*, 2012, **134**, 12320–12320.
3 A. V. Yakovenko, V. I. Boyko, V. I. Kalchenko, L. Baldini, A. Casnati, F. Sansone and R. Ungaro, *J. Org. Chem.*, 2007, **72**, 3223–3231.
4 M. Arslan, S. Sayin and M. Yilmaz, *Tetrahedron: Asymmetry*, 2013, **24**, 982–989.
5 T. Hartman, V. Herzig, M. Budšinsky, J. Jindřich, R. Cibulka and T. Kraus, *Tetrahedron: Asymmetry*, 2012, **23**, 1571–1583.
6 G. Tasnádi, E. Forró and F. Fülöp, *Tetrahedron: Asymmetry*, 2009, **20**, 1771–1777.
7 V. Mojr, V. Herzig, M. Buděšínský, R. Cibulka and T. Kraus, *Chem. Commun.*, 2010, **46**, 7599–7601.
8 E. Yilmaz, M. Sezgin and M. Yilmaz, *Biocatal. Biotransform.*, 2009, **27**, 360–366.
9 E. Yilmaz, M. Sezgin and M. Yilmaz, *J. Mol. Catal. B: Enzym.*, 2011, **69**, 35–41.
10 M. F. El-Behairy and E. Sundby, *Tetrahedron: Asymmetry*, 2013, **24**, 285–289.
11 I. Ali, N. Lahoucine, A. Ghanem and H. Y. Aboul-Enein, *Talanta*, 2006, **69**, 1013–1017.
12 E. Ozyilmaz and S. Sayin, *Appl. Biochem. Biotechnol.*, 2013, **170**, 1871–1884.
13 F. Kartal, M. H. A. Janssen, F. Hollmann, R. A. Sheldon and A. Kilinc, *J. Mol. Catal. B: Enzym.*, 2011, **71**, 85–89.
14 S. Sayin, E. Yilmaz and M. Yilmaz, *Org. Biomol. Chem.*, 2011, **9**, 4021–4024.
15 E. B. Pereira, H. F. De Castro, F. F. De Moraes and G. M. Zanin, *Appl. Biochem. Biotechnol.*, 2001, **93**, 739–752.
16 S. Takac and M. Bakkal, *Process Biochem.*, 2007, **42**, 1021–1027.
17 A. Uyanik, N. Sen and M. Yilmaz, *Bioresour. Technol.*, 2011, **102**, 4313–4318.
18 S. Erdemir and M. Yilmaz, *J. Mol. Catal. B: Enzym.*, 2009, **58**, 29–35.
19 P. Slavik, M. Dudic, K. Flidrova, J. Sykora, I. Cisarova, S. Böhm and P. Lhoták, *Org. Lett.*, 2012, **14**, 3628–3631.
20 S. Elcin and H. Deligöz, *Tetrahedron*, 2013, **69**, 6832–6838.
21 A. Casnati, *Chem. Commun.*, 2013, **49**, 6827–6830.
22 S. Sayin, G. U. Akkus, R. Cibulka, I. Stibor and M. Yilmaz, *Helv. Chim. Acta*, 2011, **94**, 481–486.
23 M. A. Qazi, Ü. Ocak, M. Ocak, S. Memon and I. B. Solangi, *J. Fluoresc.*, 2013, **23**, 575–590.
24 O. O. Karakus and H. Deligöz, *Anal. Lett.*, 2010, **43**, 768–775.
25 E. Ozyilmaz and S. Sayin, *Bioprocess Biosyst. Eng.*, 2013, **36**, 1803–1806.
26 O. Sahin, S. Erdemir, A. Uyanik and M. Yilmaz, *Appl. Catal., A*, 2009, **369**, 36–41.
27 F. Ozcan, M. Ersoz and M. Yilmaz, *Mater. Sci. Eng., C*, 2009, **29**, 2378–2383.
28 M. M. Bradford, *Anal. Biochem.*, 1976, **72**, 248–254.
29 S. H. Chiou and W. T. Wu, *Biomaterials*, 2004, **25**, 197–204.
30 M. Bonnet, C. Leroux, Y. Chilliard and P. Martin, *Mol. Cell Probes*, 2001, **15**, 187–194.
31 K. Faber, *Biocatalysis*, 1993, **8**, 91–132.
32 E. Ozyilmaz, S. Sayin, M. Arslan and M. Yilmaz, *Colloids Surf., B*, 2014, **113**, 182–189.
33 C. D. Gutsche and L. J. Bauer, *J. Am. Chem. Soc.*, 1985, **107**, 6052–6059.
34 C. S. Chen, Y. Fujimoto, G. Girdaukas and C. J. Sih, *J. Am. Chem. Soc.*, 1982, **104**, 7294–7299.
35 E. Akoz, S. Sayin and M. Yilmaz, *Appl. Biochem. Biotechnol.*, 2014, **172**, 509–523.

